

Vector Autoregressive Models with Spatially Structured Coefficients for Time Series on a Spatial Grid

Yuan Yan¹, Hsin-Cheng Huang² and Marc G. Genton³

October 11, 2024

Abstract

We propose a parsimonious spatiotemporal model for time series data on a spatial grid. Our model is capable of dealing with high-dimensional time series data that may be collected at hundreds of locations and capturing the spatial non-stationarity. In essence, our model is a vector autoregressive model that utilizes the spatial structure to achieve parsimony of autoregressive matrices at two levels. The first level ensures the sparsity of the autoregressive matrices using a lagged-neighborhood scheme. The second level performs a spatial clustering of the non-zero autoregressive coefficients such that nearby locations share similar coefficients. This model is interpretable and can be used to identify geographical subregions, within each of which, the time series share similar dynamical behavior with homogeneous autoregressive coefficients. The model parameters are obtained using the penalized maximum likelihood with an adaptive fused Lasso penalty. The estimation procedure is easy to implement and can be tailored to the need of a modeler. We illustrate the performance of the proposed estimation algorithm in a simulation study. We apply our model to a wind speed time series dataset generated from a climate model over Saudi Arabia to illustrate its usefulness. Limitations and possible extensions of our method are also discussed.

Some key words: Adaptive fused Lasso; Coefficients homogeneity; Penalized maximum likelihood; Regularization; Spatial clusters; Spatiotemporal model.

¹ Department of Mathematics & Statistics, Dalhousie University, Halifax, NS, B3H 4R2, Canada.
E-mail: yuan.yan@dal.ca

² Institute of Statistical Science, Academia Sinica, Taipei 115, Taiwan.
E-mail: hchuang@stat.sinica.edu.tw.

³ Statistics Program, King Abdullah University of Science and Technology (KAUST), Thuwal 23955-6900, Saudi Arabia.
E-mail: marc.genton@kaust.edu.sa.

This publication is based upon work supported by the King Abdullah University of Science and Technology (KAUST) Office of Sponsored Research (OSR) under Award No: OSR-2018-CRG7-3742.

1 Introduction

In this age of big data, large spatiotemporal datasets are readily available in various scientific fields. In particular, time series data collected on a high-resolution spatial grid are frequently encountered in the environmental, climate, and marine sciences. These data may be calculated from a satellite-borne instrument signal (e.g., scatterometer) or simulated from a physical model. Flexible and interpretable spatiotemporal models that are also parsimonious and computationally feasible are needed in order to understand the space-time dynamics underlying the data, make better forecasts, or generate fast simulation (stochastic weather generator) of such spatiotemporal data.

Traditional covariance-based space-time models often impose strong assumptions, such as stationarity and isotropy of the covariance function, which are not realistic for data with a sizable spatial range. Thus, the classical parametric spatiotemporal covariance modeling cannot capture the complex space-time structures of the data. Cressie and Wikle (2011) strongly recommend and prefer dynamical spatiotemporal models (DSTM) over the descriptive spatiotemporal covariance modeling. One commonly adopted linear DSTM for describing temporal dynamics is the vector autoregressive (VAR) model, where each variable corresponds to the process at one spatial location. Here, we give a brief review of a VAR(p) model in the DSTM framework. Throughout this paper, we assume $\mathbf{Z}_t = (Z_t(\mathbf{s}_1), \dots, Z_t(\mathbf{s}_n))'$ for $t = 1, \dots, T$ is a time series of a zero-mean spatial process at n locations. A Gaussian VAR(p) model of dimension n is defined as

$$\mathbf{Z}_t = \mathbf{A}_1 \mathbf{Z}_{t-1} + \dots + \mathbf{A}_p \mathbf{Z}_{t-p} + \boldsymbol{\epsilon}_t, \quad t = 2, \dots, T, \quad (1)$$

where \mathbf{A}_i are the fixed $n \times n$ matrices of autoregressive coefficients (i.e., transition matrices or propagator matrices) of order i , and $\boldsymbol{\epsilon}_t = (\epsilon_t(\mathbf{s}_1), \dots, \epsilon_t(\mathbf{s}_n))'$ is an innovation time series of spatial random effects that follows an independent and identically distributed (i.i.d.) multivariate Gaussian distribution with mean $\mathbf{0}$ and covariance matrix $\boldsymbol{\Psi}$, $\boldsymbol{\epsilon}_t \stackrel{i.i.d.}{\sim} \mathcal{N}_n(\mathbf{0}, \boldsymbol{\Psi})$, and $\boldsymbol{\Psi}$ could be modeled by some commonly used parametric spatial covariance function.

The spatial setting for a VAR model can be both a curse and a blessing. On the one hand, for time series obtained at n gridded locations, the number of parameters, n^2 , for each transition matrix \mathbf{A}_i can be enormous, which makes estimation difficult and unstable, if not impossible. On the other hand, by taking advantage of the spatial structure, parsimony assumptions can be made for the transition matrices. In this paper, we develop a model for time series on a spatial grid where the parsimony of our model is enforced at two levels. First, the sparsity of each \mathbf{A}_i is obtained by using a lagged-neighborhood scheme for given K_i neighbors. Then the non-zero coefficients in \mathbf{A}_i can be interpreted as the influence or flow from a neighbor in a certain direction at time lag i . Second, we assume the non-zero coefficients are clustered in space such that within some subregions nearby locations share the same or similar autoregressive coefficients while across different subregions the coefficients may have distinct values. Our model is capable of dealing with high-dimensional time series data collected at hundreds of locations and is especially helpful when the time series data are rich in space but not long in time. In such situations, the parameters estimated by the usual least-squares or likelihood-based methods suffer from high variances and low interpretability. Instead, we suggest a parameter-estimation method for our model based on the log-likelihood with an adaptive fused Lasso penalty to capture the coefficients homogeneity within subregions, which is easy to implement. The originality of our model truly lies in the combination of sparsity, coefficients homogeneity, and the estimation procedure, which makes the model flexible, interpretable and especially useful to identify spatial subregions.

In Section 2, we put the two-level parsimony assumption of our VAR model in the context of related and alternative modeling strategies in the literature. In Section 3, we formalize our parsimonious model for the VAR(1) case, develop the parameter-estimation method, and provide asymptotic properties of the penalized estimation. In Section 4, we demonstrate the performance of our estimation algorithm for our model in a simulation study. In Section 5, we apply our model to a daily wind speed dataset on a grid covering Saudi Arabia generated from a climate model in

order to illustrate its usefulness. Limitations and possible extensions of our model are discussed in Section 6. Proofs can be found in the Appendix.

2 Literature Review

For the first level, our VAR model adopts a lagged-neighborhood scheme for a pre-specified number of neighbors which endows each \mathbf{A}_i with some given sparsity structure. Assumption of fixed sparsity structure for the transition matrices is simple while sensible and was adopted by multiple authors. Rao (2008) introduced a VAR(p) model with a diagonal structure for each \mathbf{A}_i . The hierarchical model in Wikle et al. (1998) included a VAR(1) process with a lagged-nearest-neighbor scheme for the transition matrix and was applied to the analysis of monthly averaged maximum-temperature data. The lagged-nearest-neighbor scheme takes into account influence by the studied location itself and its four nearest neighbors. Tagle et al. (2019) adopted a VAR(2) process with a lagged-nearest-neighbor scheme for \mathbf{A}_1 and a diagonal structure for \mathbf{A}_2 to analyze wind speed data.

Instead of a fixed sparsity structure, a more flexible sparsity structure on the VAR transition matrices based on the data can be achieved by a variable selection/model building scheme or a penalized likelihood method. de Luna and Genton (2005) proposed a variable selection procedure carried out at each location separately in which the variables (locations) were ordered based on their relative distances (or importance, when additional information is available) from the location under study. First, they defined a spatial partial correlation function with respect to the order; then, they selected the model from the sample partial correlation functions, similarly to the order selection by checking the partial autocorrelation function (PACF) in the time series context. Hsu et al. (2008) adopted the Lasso penalty for subset selection in a VAR model and estimated the non-zero coefficients simultaneously for a better forecasting performance. Basu and Michailidis (2015) provided a theoretical justification for estimating the VAR models with the Lasso penalty. By taking advantage of the spatial configuration, Ngueyep and Serban

(2015) used a weighted L_1 penalty as a function of the spatial distance between two locations for multilayer spatial VAR. Monbet and Ailliot (2017) applied the smoothly clipped absolute deviation (SCAD) penalty to facilitate a sparse structure on both the transition matrices and the precision matrix (Ψ^{-1}) for the innovation process. Schweinberger et al. (2017) developed a two-step L_1 penalized least squares method to capture the sparsity structure of the transition matrices based on distance.

Other approaches to reduce the number of parameters involved in a spatial VAR include parametric modeling of the transition matrices and possibly combined with dimension reduction. Ailliot et al. (2006) employed a VAR(1) model for wind fields with a latent process that described the motion of the air masses. In that physically-driven model, \mathbf{A}_1 and Ψ were both parameterized as a function of the latent translation of the wind fields. Wikle et al. (2001) and Katzfuss and Cressie (2012) implemented a dimension reduction technique with spatial basis functions, and modeled the resulting lower-dimensional process using a VAR(1) model, where the transition matrix had a parametric block structure related to the spatial resolution of the spatial bases. Bessac et al. (2015) built a spatiotemporal model in the state-space form, where the process at all points depended on a common univariate state variable, which was an AR(1) time series and contained large-scale spatial variation (regional information). Finally, in econometrics, there is a vast literature on Bayesian VAR with different shrinkage priors on the vectorized transition matrices for high-dimensional VAR models (e.g., Bańbura et al., 2010; Korobilis and Pettenuzzo, 2019).

For the second level, our model assumes the non-zero coefficients that represent the influence from a neighbor in a certain direction are region-wise constant. Then, the dynamics of the process are the same within each subregions and are allowed to vary discontinuously across different subregions possibly with distinct geographical features. The novelty of our model is essentially to extend the pursuit of homogeneity in coefficients to the spatial VAR setting. Previously, for linear regression, in order to identify homogeneous groups of predictors, Shen and Huang (2010) used a

nonconvex and overcomplete penalty on pairwise differences of the coefficients. Ke et al. (2015) proposed a two-step procedure to first have preliminary ordered segments of the coefficients and then penalize the pairwise differences of the coefficients between adjacent segments and within individual segments. When the predictors are naturally ordered, it becomes the fused Lasso method proposed by Tibshirani et al. (2005). The method penalizes the successive differences among the coefficients to achieve local constancy of the coefficients. Zou (2006) introduced the adaptive Lasso, by giving different weights for different penalty terms. Sun et al. (2016) used adaptive fused Lasso to estimate spatial and temporal quantile functions with spatially and temporally homogeneous groups, respectively. Under the spatial regression setting, Huang et al. (2010) proposed the spatial Lasso with homogeneous coefficients given known subregion structure. Recently, to identify the spatially clustered patterns in the coefficients, Li and Sang (2019) used the fused Lasso penalty on edges of the minimum spanning tree formed by the spatial locations, while Kazar and Hering (2019) proposed the Markov random field finite mixture regression model.

Rather than the homogeneity approach, VAR models with smoothly varying diagonal coefficients were considered in Rao (2008) and Wikle et al. (1998). Rao (2008) let the diagonal coefficients vary smoothly in space which are estimated by localized least squares, in order to accommodate for the spatial non-stationarity of the process and to allow spatial interpolation; while in Wikle et al. (1998), the diagonal coefficients varied spatially according to a conditionally autoregressive (CAR) model for the spatial lattice while coefficients related to the four nearest neighbors are kept constant over space. These models are related to the geographically weighted regression (GWR) (Brunsdon et al., 1996) and spatially varying coefficient processes (Gelfand et al., 2003) under the spatial regression setting.

3 Model, Estimation, and Properties

3.1 The Spatiotemporal VAR(1) Model

We formalize our model for the VAR(1) case. We let $D_s \subset \mathbb{R}^2$ be gridded locations, $D_s = \{\mathbf{s}_1, \dots, \mathbf{s}_n\} \subset \{(i_1, i_2) : i_1 = 1, \dots, n_x, i_2 = 1, \dots, n_y\}$. We assume that for location \mathbf{s}_i , $Z_t(\mathbf{s}_i)$ is directly affected only by the lag-1 process at the K neighboring locations (including the location itself) $Z_{t-1}(\mathbf{s}_i + \mathbf{u}_k), k = 1, \dots, K$, for some translation vector \mathbf{u}_k . For example, if $\mathbf{u}_k = (-1, 0)'$, then $\mathbf{s}_i + \mathbf{u}_k$ is the left neighbor of \mathbf{s}_i , and we fix $\mathbf{u}_1 = \mathbf{0}$ to always include the location \mathbf{s}_i itself. For a finite grid, boundary conditions are required when $\mathbf{s}_i + \mathbf{u}_k \notin D_s$. We are only interested in coefficients and dynamics for the n_I inner grid points, for each of which all K neighbors are within D_s . A simple model can be assumed for the $n_B = n - n_I$ boundary points in order to simulate data on the boundary. For easy notation, we order the grid points such that the first n_I points \mathbf{s}_i for $i = 1, \dots, n_I$ are the inner grid points. We adopt the lagged-neighborhood scheme only for these inner grid points; for the boundary grid points, we set $K = 1$ so that their temporal evolution depends only on themselves. Our model can be expressed as

$$\begin{aligned} Z_t(\mathbf{s}_i) &= \sum_{k=1}^K \alpha_k(\mathbf{s}_i) Z_{t-1}(\mathbf{s}_i + \mathbf{u}_k) + \epsilon_t(\mathbf{s}_i), & i = 1, \dots, n_I, t = 2, \dots, T, \\ Z_t(\mathbf{s}_i) &= \alpha_1(\mathbf{s}_i) Z_{t-1}(\mathbf{s}_i) + \epsilon_t(\mathbf{s}_i), & i = n_I+1, \dots, n, t = 2, \dots, T, \end{aligned} \quad (2)$$

where $\epsilon_t \stackrel{i.i.d.}{\sim} \mathcal{N}_n(\mathbf{0}, \Psi)$ and $\alpha_k(\mathbf{s}_i)$ corresponds to the influence by the k th neighbor to the process at \mathbf{s}_i . The lagged-nearest-neighbor scheme in Wikle et al. (1998) and Tagle et al. (2019) corresponds to the case when $K = 5$, which captures the influence from the location itself and its four nearest neighbors. These five locations on a grid may be referred to as the five-point stencil in the numerical analysis literature, the first-order stencil neighborhood scheme in high-performance computing, and as the rook's neighbor or the first-order neighborhood elsewhere. It can be easily extended to the second-order neighborhood with $K = 9$ (queen's neighbor), which includes the nearest eight neighbors and the location itself. More flexibly, \mathbf{u}_k in (2) can be selected based on prior knowledge of the spatiotemporal process and the choice is not limited

to the K -nearest neighbors. For example, if a river flows to the east, then it is sensible to model the chemical concentration at a location in the river to depend on only its western neighbors.

For each $k = 1, \dots, K$, we let $\boldsymbol{\alpha}_k = (\alpha_k(\mathbf{s}_1), \dots, \alpha_k(\mathbf{s}_{n_I}))'$ be the vector of the unknown parameters of interest, which are the coefficients related to the k th neighbor for each of the n_I inner grid points. Let $\boldsymbol{\alpha}_B = (\alpha_1(\mathbf{s}_{n_I+1}), \dots, \alpha_1(\mathbf{s}_n))'$ be the vector of the unknown autoregressive coefficients of the boundary points. Time series of a spatial process often have some regional structure such that locations within one region share the same spatiotemporal dynamics while the dynamics could vary discontinuously across different subregions. Therefore, a spatial coefficient-grouping structure such that $\boldsymbol{\alpha}_k$ is composed of spatial clusters of values for each $k = 1, \dots, K$ is desirable. We assume no spatial structure for $\boldsymbol{\alpha}_B$; these coefficients are of little practical importance and are only modeled to allow forecasting several steps ahead and to simplify notations. Figure 1 of our simulation design gives an intuitive visual illustration of the idea of spatial homogeneity in the autoregressive coefficients.

The model defined by (2) can be written as the VAR model in (1) with order $p = 1$ and $\mathbf{A}_1 = \mathbf{A}$. We let a_{ij} be the (i, j) th entry of \mathbf{A} . With the lagged-neighborhood scheme, \mathbf{A} has a sparse form such that $a_{ij} \neq 0$, only if $\mathbf{s}_j = \mathbf{s}_i + \mathbf{u}_k$ for some k and there are at most a total of $m = Kn_I + n_B$ non-zero elements in \mathbf{A} . Since the sparsity of \mathbf{A} is combined with the spatial clustered structure of each $\boldsymbol{\alpha}_k$, the reduction in the number of parameters is drastic compared to the n^2 parameters required by the full VAR(1) model. We let $\boldsymbol{\alpha} = (\boldsymbol{\alpha}'_1, \dots, \boldsymbol{\alpha}'_K, \boldsymbol{\alpha}'_B)'$ be the vector of all the unknown coefficients of length m ; then, the sparse transition matrix \mathbf{A} depends only on $\boldsymbol{\alpha}$ through $\text{vec}(\mathbf{A}) = \mathbf{P}\boldsymbol{\alpha}$, where \mathbf{P} is a $n^2 \times m$ matrix of zeros and ones that indicates the positions of the corresponding non-zero elements in $\text{vec}(\mathbf{A})$ for $\boldsymbol{\alpha}$.

The VAR(1) time series $\{\mathbf{Z}_t\}$ is stable if the roots of $|\mathbf{I}_n - \mathbf{A}z| = 0$ all lie outside $\{z \in \mathbb{C} : |z| \leq 1\}$ or, equivalently, any eigenvalue of \mathbf{A} has a modulus less than 1. The following lemma ensures stability.

Lemma 1. *Consider the model given by (1) with $p=1$. Suppose that $\sum_{j=1}^n |a_{ij}| < 1$, $i = 1, \dots, n$,*

where a_{ij} is the (i, j) th entry of \mathbf{A} , $i, j = 1, \dots, n$. Then, the time series $\{\mathbf{Z}_t\}$ given by (1) is stable.

The proof of Lemma 1 can be found in the Appendix. From Lemma 1, we can ensure stability for our VAR(1) model by imposing the constraint $\sum_{k=1}^K |\alpha_k(\mathbf{s}_i)| < 1$ for $i = 1, \dots, n_I$, and $|\alpha_1(\mathbf{s}_i)| < 1$ for $i = n_I + 1, \dots, n$.

3.2 Parameter Estimation by the Adaptive Fused Lasso

For our model, the dynamical spatiotemporal coefficients $\boldsymbol{\alpha}$ and the matrix $\boldsymbol{\Psi}$ that models the spatial covariance need to be estimated. To capture the spatial homogeneous groups of $\boldsymbol{\alpha}$, a penalized likelihood method is appropriate. For parameter estimation in our model, we consider the adaptive fused Lasso penalty. Tibshirani and Taylor (2011) developed a path algorithm for a ‘generalized’ Lasso problem that included the Lasso, fused Lasso, and adaptive Lasso as special cases. This generalized Lasso problem can be solved efficiently and is easy to implement using the ‘genlasso’ package (Arnold and Tibshirani, 2014) in R (R Development Core Team, 2019).

We consider the conditional log-likelihood of $\mathbf{Z}_2, \dots, \mathbf{Z}_T$ conditioning on \mathbf{Z}_1 for our model with $\boldsymbol{\Psi}$ given. For any matrix \mathbf{X} and vector \mathbf{y} that satisfy

$$\mathbf{X}'\mathbf{X} = \mathbf{P}' \left\{ \left(\sum_{t=2}^T \mathbf{Z}_{t-1} \mathbf{Z}_{t-1}' \right) \otimes \boldsymbol{\Psi}^{-1} \right\} \mathbf{P}, \quad (3)$$

$$\mathbf{X}'\mathbf{y} = \mathbf{P}' \text{vec} \left(\boldsymbol{\Psi}^{-1} \sum_{t=2}^T \mathbf{Z}_t \mathbf{Z}_{t-1}' \right), \quad (4)$$

the conditional log-likelihood can be written as a second-order polynomial of $\boldsymbol{\alpha}$ (the proof can be found in the Appendix):

$$l(\boldsymbol{\alpha}) = -\frac{1}{2} \sum_{t=2}^T (\mathbf{Z}_t - \mathbf{A} \mathbf{Z}_{t-1})' \boldsymbol{\Psi}^{-1} (\mathbf{Z}_t - \mathbf{A} \mathbf{Z}_{t-1}) = -\frac{1}{2} \|\mathbf{y} - \mathbf{X} \boldsymbol{\alpha}\|_2^2 + \text{constant}, \quad (5)$$

where $\|\cdot\|_2$ is the ℓ_2 -norm. One way to choose \mathbf{X} is to compute the Cholesky decomposition of the matrix on the right-hand side of (3) and, then, solve for \mathbf{y} from (4).

We consider a penalized maximum likelihood (PML) method with the following objective function:

$$F(\boldsymbol{\alpha}) = l(\boldsymbol{\alpha}) - \lambda \sum_{k=1}^K \sum_{i \sim j} w_{k,i,j} |\alpha_k(\mathbf{s}_i) - \alpha_k(\mathbf{s}_j)|, \quad (6)$$

where the last term is an adaptive fused Lasso penalty for a two-dimensional grid that facilitates the grouping of neighboring coefficients, $i \sim j$ denotes that \mathbf{s}_i is a direct neighbor of \mathbf{s}_j (there is an edge between \mathbf{s}_i and \mathbf{s}_j on the grid), for $i, j = 1, \dots, n_I$, λ is a tuning parameter that controls the degree of grouping, and $\{w_{k,i,j}\}$ are known weight values set to $w_{k,i,j} = |\tilde{\alpha}_k(\mathbf{s}_i) - \tilde{\alpha}_k(\mathbf{s}_j)|^{-\gamma}$, where $\tilde{\boldsymbol{\alpha}}$ is a root- T consistent estimator of $\boldsymbol{\alpha}$ and γ is some fixed positive constant. We penalize the pairwise difference of $\alpha_k(\cdot)$ between direct neighbors within the inner grid points. For each $k = 1, \dots, K$, the number of penalty terms equals to the number of edges in the inner grid. Instead of the extensive pairwise difference penalty used by Shen and Huang (2010) or the difference between the coefficient of a location and the average of its neighboring coefficients used by Sun et al. (2016), we take advantage of the spatial configuration and penalize on ‘just enough’ pairs for coefficients clustering. The maximization problem (6), given $\boldsymbol{\Psi}$, is a generalized Lasso problem,

$$\min_{\boldsymbol{\alpha}} \left\{ \frac{1}{2} \|\mathbf{y} - \mathbf{X}\boldsymbol{\alpha}\|_2^2 + \lambda \|\mathbf{D}\boldsymbol{\alpha}\|_1 \right\}, \quad (7)$$

where $\|\cdot\|_1$ is the ℓ_1 -norm for some penalty matrix \mathbf{D} determined by the structure of the grid and $w_{k,i,j}$. The neighborhood structure of $\boldsymbol{\alpha}$ given by (6) and (7) corresponds to a graph formed by K disjoint subgraphs with the same grid structure; K determines the level of sparsity for \mathbf{A} , while the penalty on pairwise difference between direct neighbors assists in capturing the spatial homogeneity of the VAR coefficients.

When $\lambda = 0$, the solution of (7) corresponds to the restricted generalized least squares (GLS) estimator of \mathbf{A} . As $\lambda \rightarrow \infty$, $\alpha_k(\cdot)$ reduces to a constant function because the network corresponding to $\{\mathbf{s}_i : i = 1, \dots, n_I\}$ is connected. A proper tuning parameter λ can be selected by 5-fold cross validation (Bergmeir and Bentez, 2012) or by the Bayesian information criterion (BIC), $\text{BIC}(\lambda) = \|\mathbf{y} - \mathbf{X}\boldsymbol{\alpha}_\lambda\|_2^2 + \log(T-1)\text{df}(\mathbf{X}\boldsymbol{\alpha}_\lambda)$, where $\boldsymbol{\alpha}_\lambda$ is the solution to the generalized

Lasso problem in (7) for a given λ , and $\text{df}(\mathbf{X}\boldsymbol{\alpha}_\lambda)$ can be estimated from the number of distinct values in $\boldsymbol{\alpha}_\lambda$ (Tibshirani and Taylor, 2011).

Given $\boldsymbol{\alpha}$ and the corresponding \mathbf{A} , we estimate $\boldsymbol{\Psi}$ using the maximum likelihood estimator:

$$\hat{\boldsymbol{\Psi}} = \frac{1}{T-1} \sum_{t=2}^T (\mathbf{Z}_t - \mathbf{A}\mathbf{Z}_{t-1})'(\mathbf{Z}_t - \mathbf{A}\mathbf{Z}_{t-1}). \quad (8)$$

We propose the following algorithm for estimating $\boldsymbol{\alpha}$ and $\boldsymbol{\Psi}$ iteratively in three steps to get the adaptive fused Lasso estimator. We start with the restricted ordinary least squares (OLS) estimator $\hat{\mathbf{A}}^{(0)}$ of \mathbf{A} with $\boldsymbol{\Psi} = \mathbf{I}_n$ in (5) and use the residuals $\mathbf{Z}_t - \hat{\mathbf{A}}^{(0)}\mathbf{Z}_{t-1}$ to get an estimator of $\boldsymbol{\Psi}$ from (8). In step II, we solve the PML (7) with uniform weights and λ selected by the Bayesian information criterion (BIC) to get the fused Lasso estimator. The GLS estimator could be obtained by setting $\lambda = 0$ in step II. Finally in step III, we compute weights from the fused Lasso estimator and obtain the adaptive fused Lasso estimator.

ALGORITHM:

1. Step I: Initial estimation using the restricted ordinary least squares (OLS)
 - (a) Fix $\boldsymbol{\Psi} = \hat{\boldsymbol{\Psi}}^{(0)} = \mathbf{I}_n$, solve (7) with $\lambda = 0$ to get $\hat{\boldsymbol{\alpha}}^{(0)}$ and the corresponding $\hat{\mathbf{A}}^{(0)}$, which is the restricted OLS estimator of \mathbf{A} with the constraints that $a_{ij} = 0$ except for the m parameters corresponding to $\boldsymbol{\alpha}$;
 - (b) Fix $\mathbf{A} = \hat{\mathbf{A}}^{(0)}$ and get $\hat{\boldsymbol{\Psi}}^{(1)}$ from (8);
2. Step II: Fused Lasso
 - (a) Fix $\boldsymbol{\Psi} = \hat{\boldsymbol{\Psi}}^{(1)}$ and set $w_{k,i,j} \equiv 1$, to obtain the fused Lasso estimator of $\hat{\boldsymbol{\alpha}}^{(1)}$ and the corresponding $\hat{\mathbf{A}}^{(1)}$ by solving (7) with λ selected by BIC;
 - (b) Fix $\mathbf{A} = \hat{\mathbf{A}}^{(1)}$ and get $\hat{\boldsymbol{\Psi}}^{(2)}$ from (8);
3. Step III: Adaptive fused Lasso
 - (a) Fix $\boldsymbol{\Psi} = \hat{\boldsymbol{\Psi}}^{(2)}$ and update $w_{k,i,j} = |\hat{\alpha}_k^{(1)}(\mathbf{s}_i) - \hat{\alpha}_k^{(1)}(\mathbf{s}_j)|^{-1}$, to obtain the adaptive fused Lasso estimator $\hat{\boldsymbol{\alpha}}$ and the corresponding $\hat{\mathbf{A}}$ by solving (7) with λ selected by BIC;
 - (b) Fix $\mathbf{A} = \hat{\mathbf{A}}$ and get $\hat{\boldsymbol{\Psi}}$ from (8).

3.3 Asymptotic Properties

Some notations are needed to state the asymptotic properties. We consider an undirected graph $\mathcal{G} = (\mathcal{V}, \mathcal{E})$, where $\mathcal{V} = \{1, \dots, m\}$ is a set of vertices corresponding to the $m = Kn_I + n_B$ parameters in $\boldsymbol{\alpha}$ to be estimated, and $\mathcal{E} \subset \mathcal{V} \times \mathcal{V}$ is a set of undirected edges that depends on the structure of the spatial grid. Here \mathcal{V} can be partitioned into $n_B + K$ disjoint components, including n_B isolated nodes (corresponding to the non-regularized coefficients in $\boldsymbol{\alpha}_B$) and K identical disjoint components each with n_I vertices and the same inner grid structure (corresponding to the penalized coefficients in $\boldsymbol{\alpha}_k$, for $k = 1, \dots, K$). With these notations, the penalty term in (6) can be rewritten as

$$\lambda \sum_{k=1}^K \sum_{i \sim j} w_{k,i,j} |\alpha_k(\mathbf{s}_i) - \alpha_k(\mathbf{s}_j)| = \lambda \sum_{(i,j) \in \mathcal{E}} w_{i,j} |\alpha_i - \alpha_j|,$$

where $w_{i,j} = |\tilde{\alpha}_i - \tilde{\alpha}_j|^{-\gamma}$.

We let $\boldsymbol{\alpha}^0$ be the true parameter vector and define $\boldsymbol{\xi} = \mathbf{y} - \mathbf{X}\boldsymbol{\alpha}^0$. We introduce $\mathcal{A} = \{(i, j) \in \mathcal{E} : \alpha_i^0 = \alpha_j^0, i, j = 1, \dots, n_I\}$ and consider the subgraph $\mathcal{G}_{\mathcal{A}} = (\mathcal{V}, \mathcal{A})$ of \mathcal{G} . We denote by m_0 the number of its connected components, that is the number of distinct values in $\boldsymbol{\alpha}^0$ supported by \mathcal{G} . We further denote by $\mathcal{V}_1, \dots, \mathcal{V}_{m_0}$ the sets of nodes of each connected components of $\mathcal{G}_{\mathcal{A}}$ and set $l_i = \min \mathcal{V}_i$ for $i = 1, \dots, m_0$. We define $\boldsymbol{\alpha}_{\mathcal{A}}^0 = (\alpha_{l_1}^0, \dots, \alpha_{l_{m_0}}^0)'$ and $\mathbf{X}_{\mathcal{A}}$ a matrix whose i -th column, for $i = 1, \dots, m_0$, is $\mathbf{X}_{\mathcal{A}_i} = \sum_{j \in \mathcal{V}_i} \mathbf{X}_j$, where \mathbf{X}_j is the j -th column of \mathbf{X} . We assume that $\mathbf{X}'\mathbf{X}/(T-1) \rightarrow \mathbf{C}$ as $T \rightarrow \infty$ for some positive-definite $m \times m$ matrix \mathbf{C} , which depends on $\boldsymbol{\alpha}^0$ and $\boldsymbol{\Psi}$. We denote by $\mathbf{C}_{\mathcal{A}}$ the limiting $m_0 \times m_0$ matrix of $\mathbf{X}'_{\mathcal{A}}\mathbf{X}_{\mathcal{A}}/(T-1)$ as $T \rightarrow \infty$.

We derive the asymptotic properties of the adaptive Lasso estimator $\hat{\boldsymbol{\alpha}}$ from solving (7). We let $\mathcal{A}_n = \{(i, j) \in \mathcal{E} : \hat{\alpha}_i = \hat{\alpha}_j, i, j = 1, \dots, n_I\}$ and $\hat{\boldsymbol{\alpha}}_{\mathcal{A}} = (\hat{\alpha}_{l_1}, \dots, \hat{\alpha}_{l_{m_0}})'$.

Theorem 1. *Suppose that $\lambda/\sqrt{T} \rightarrow 0$, $\lambda T^{(\gamma-1)/2} \rightarrow \infty$, and $\mathbf{C} = \lim_{T \rightarrow \infty} \mathbf{X}'\mathbf{X}/(T-1)$ is positive-definite. Then as $T \rightarrow \infty$, the following are satisfied by the adaptive Lasso estimator $\hat{\boldsymbol{\alpha}}$:*

1. *Consistency in grouping:* $\Pr(\mathcal{A}_n = \mathcal{A}) \rightarrow 1$.

2. *Asymptotic normality:* $\sqrt{T}(\hat{\alpha}_{\mathcal{A}} - \alpha_{\mathcal{A}}^0) \xrightarrow{d} \mathcal{N}_{m_0}(\mathbf{0}, \mathbf{C}_{\mathcal{A}}^{-1})$.

The proof of Theorem 1 can be found in the Appendix.

4 Simulation Study

4.1 Simulation Design

We examine the performance of our estimation algorithm in a simulation study. We simulate time series data on a 7×7 grid ($n = 49$) in a unit square from our model (2) with $T \in \{100, 500\}$ and $K = 5$, where $\alpha = (\alpha'_1, \dots, \alpha'_5, \alpha'_B)'$ and the corresponding \mathbf{A} are shown in Figure 1. The spatial random effect ϵ_t is generated from a multivariate Gaussian distribution with mean $\mathbf{0}$, and the covariance matrix Ψ is determined from an exponential covariance function with unit variance and a range parameter of 0.25. For this 7×7 square grid, we have $n_I = 25, n_B = 24$, and thus, $m = 149$ for the length of α . We design the structure of α such that $\{\alpha'_1, \dots, \alpha'_5\}$ have

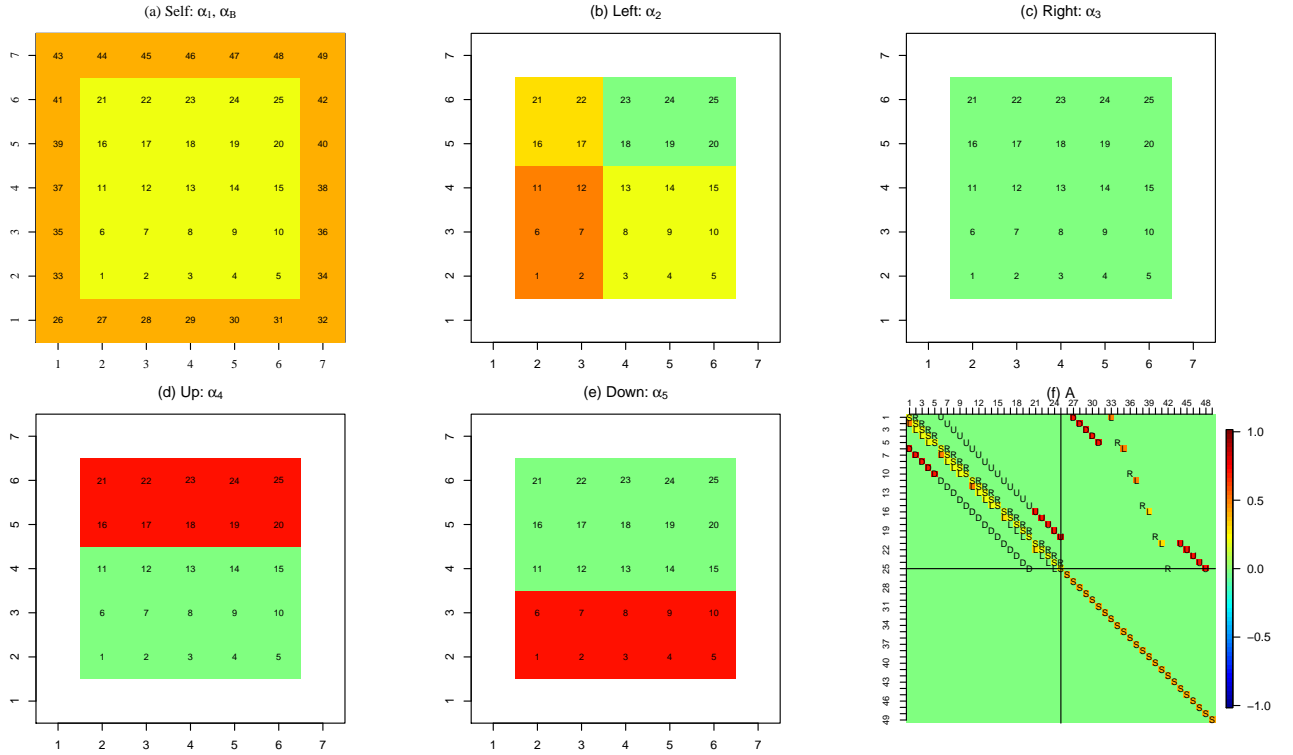


Figure 1: (a) Values of α_1 (yellow) and α_B (orange), and the indices of the 7×7 grid; (b) values of α_2 ; (c) values of α_3 ; (d) values of α_4 ; (e) values of α_5 ; (f) values of \mathbf{A} with its elements corresponding to the indices in (a).

different numbers of clusters (i.e., distinct elements). For example, α_4 and α_5 corresponding to the neighbors above and below have two clusters, α_2 corresponding to the left neighbor has four clusters, α_1 corresponding to the location itself is a constant vector, and α_3 corresponding to the right neighbor is $\mathbf{0}$.

We estimate \mathbf{A} and Ψ using the proposed algorithm given in steps I-III at the end of Section 3.2 to get the adaptive fused Lasso estimator (in step III). For comparison, we consider the restricted OLS estimator $\hat{\alpha}^0$ (in step I), the restricted GLS estimator with $\lambda = 0$ (in step II(a)), and the fused Lasso estimator $\hat{\alpha}^1$ (in step II(a)) of our algorithm.

4.2 Estimation Results

Even though the structure of the coefficients is best illustrated two-dimensionally as in Figure 1, we can ‘stretch’ (vectorize) them into a single vector ordered by the labels in each panel of Figure 1. Then, we use a functional boxplot (Sun and Genton, 2011) to visualize the performance of the estimators based on 500 simulation replicates. Figure 2 shows the functional boxplots for the estimated coefficients of five neighbors (in five rows) and the four methods (in four columns).

From Figure 2, we see that both the fused Lasso and the adaptive fused Lasso estimators have much smaller variances and are, therefore, more stable than the restricted OLS and GLS estimators. Comparing the median curves of each plot, we see that the non-regularized methods do not reproduce the structure of the coefficients, while the fused Lasso and the adaptive fused Lasso both capture the grouping of the coefficients very well. There is a small departure of the median curves from the green lines for the fused Lasso. The adaptive fused Lasso fixes this bias problem.

Although $\alpha_3 = \mathbf{0}$, the estimates of α_3 from our (adaptive) fused Lasso are only very close to but not exactly zeros. Tibshirani et al. (2005) used a sparse fused Lasso that penalized both the coefficients and the pairwise differences of the coefficients to enforce both sparsity and grouping. However, in our algorithm, we only penalize the pairwise differences, not the coefficients themselves. In an extra simulation, we used the sparse fused Lasso estimator, which

can also be written in the form of (7), where \mathbf{D} has Kn_I additional rows added to penalize the coefficients themselves. We found that our adaptive fused Lasso method without the Lasso sparsity penalization not only performs as good as the sparse fused Lasso method, but it is also computationally more efficient.

Though the choice of K might seem subjective, we can always use a larger K until the residuals pass the standard model validation procedure for a VAR model. Using a larger K increases the computational effort, but does not significantly affect the performance of the non-zero coefficients since the adaptive fused Lasso already enforces sparsity in the coefficients. Figure 3 shows estimation results with $K = 9$ in the same simulation design as described before. Comparing Figure 2 and Figure 3, we see that the estimates of $\boldsymbol{\alpha}_k, k = 1, \dots, 5$, by the fused Lasso and the adaptive fused Lasso are similar to those with $K = 5$, whereas the variances of the unregularized estimators by the restricted OLS and the restricted GLS are slightly expanded. Functional boxplots of the estimated $\boldsymbol{\alpha}_k$ (where the true $\boldsymbol{\alpha}_k$ is $\mathbf{0}$) for $k = 6, \dots, 9$, are shown in Figure 4. Again, we see the restricted OLS estimates and the restricted GLS estimates have high variances, whereas both the fused Lasso and the adaptive fused Lasso can capture the sparsity in $\boldsymbol{\alpha}$ much better.

The estimation of $\boldsymbol{\Psi}$ is intrinsically two-dimensional; therefore, we resort to the surface boxplot (Genton et al., 2014) to demonstrate the results. Figure 5 shows a surface boxplot for the proposed estimator of $\boldsymbol{\Psi}$ based on 500 simulation replicates. We see that the median image is very close to the true structure, even though our method is somewhat non-parametric.

This simulation study shows that the structure of the coefficients in our model can be captured and estimated quite well by the proposed estimation algorithm, despite the fairly small number of time points T relative to the number of parameters $n^2 + n(n + 1)/2$ to be estimated for a conventional VAR(1) model with dimension n .

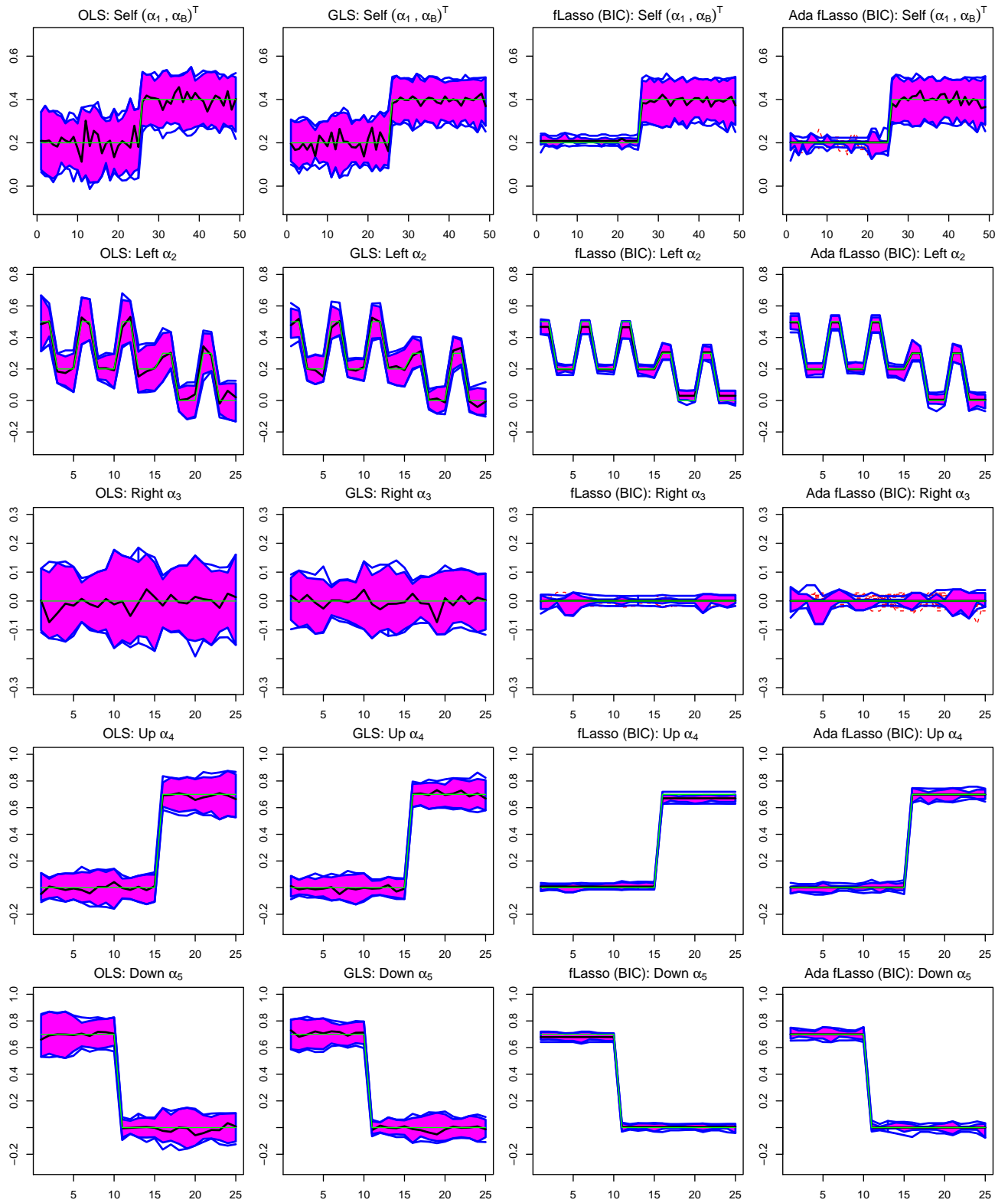


Figure 2: Functional boxplots of the estimated α_k , $k = 1, \dots, 5$ using restricted OLS, restricted GLS, fused Lasso, and adaptive fused Lasso methods with $K = 5$ and $T = 500$ from 500 simulations. True values for α_k are indicated by the green line.

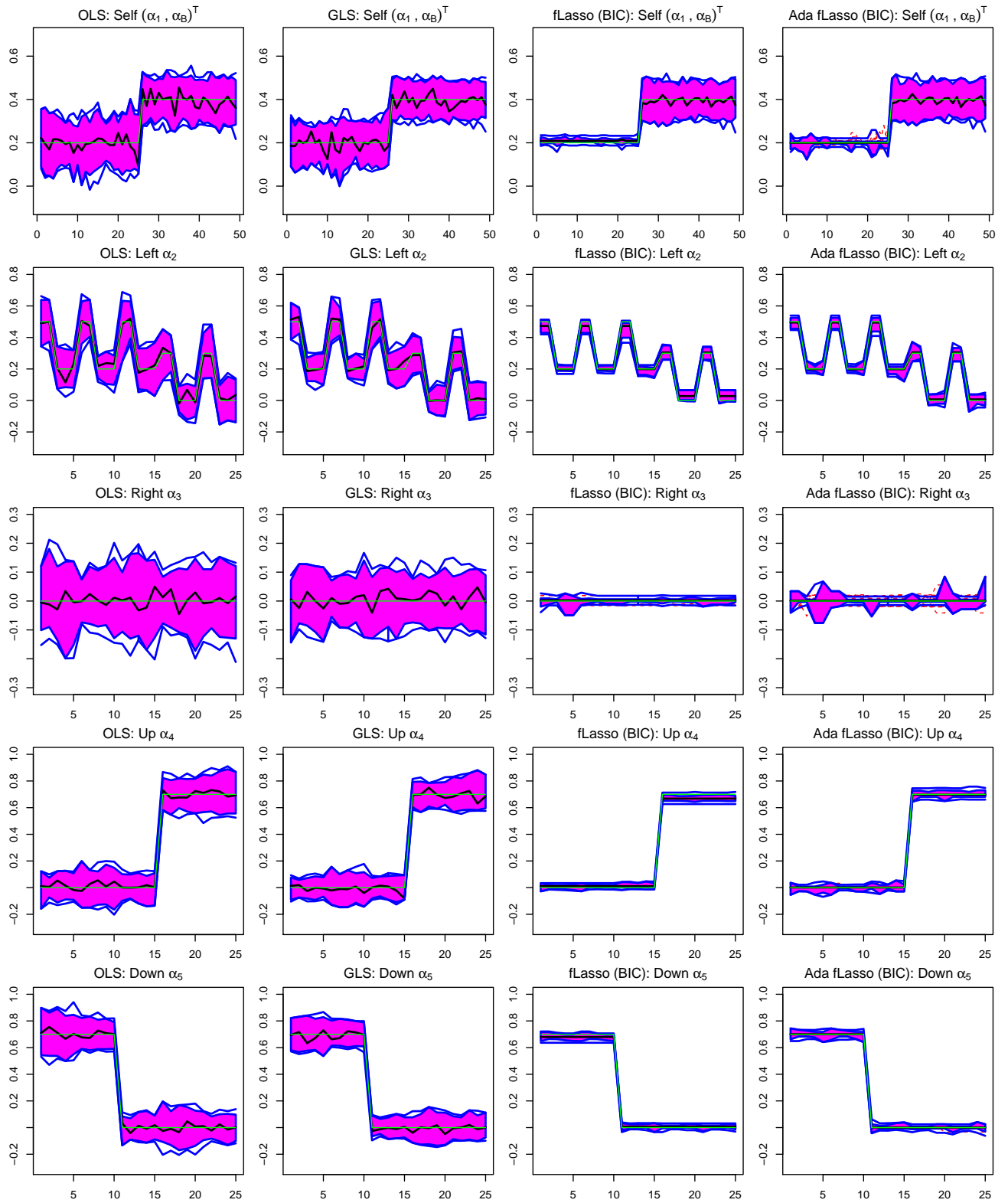


Figure 3: Functional boxplots of the estimated α_k , $k = 1, \dots, 5$ using restricted OLS, restricted GLS, fused Lasso, and adaptive fused Lasso methods with $K = 9$ and $T = 500$ from 500 simulations. True values for α_k are indicated by the green line.

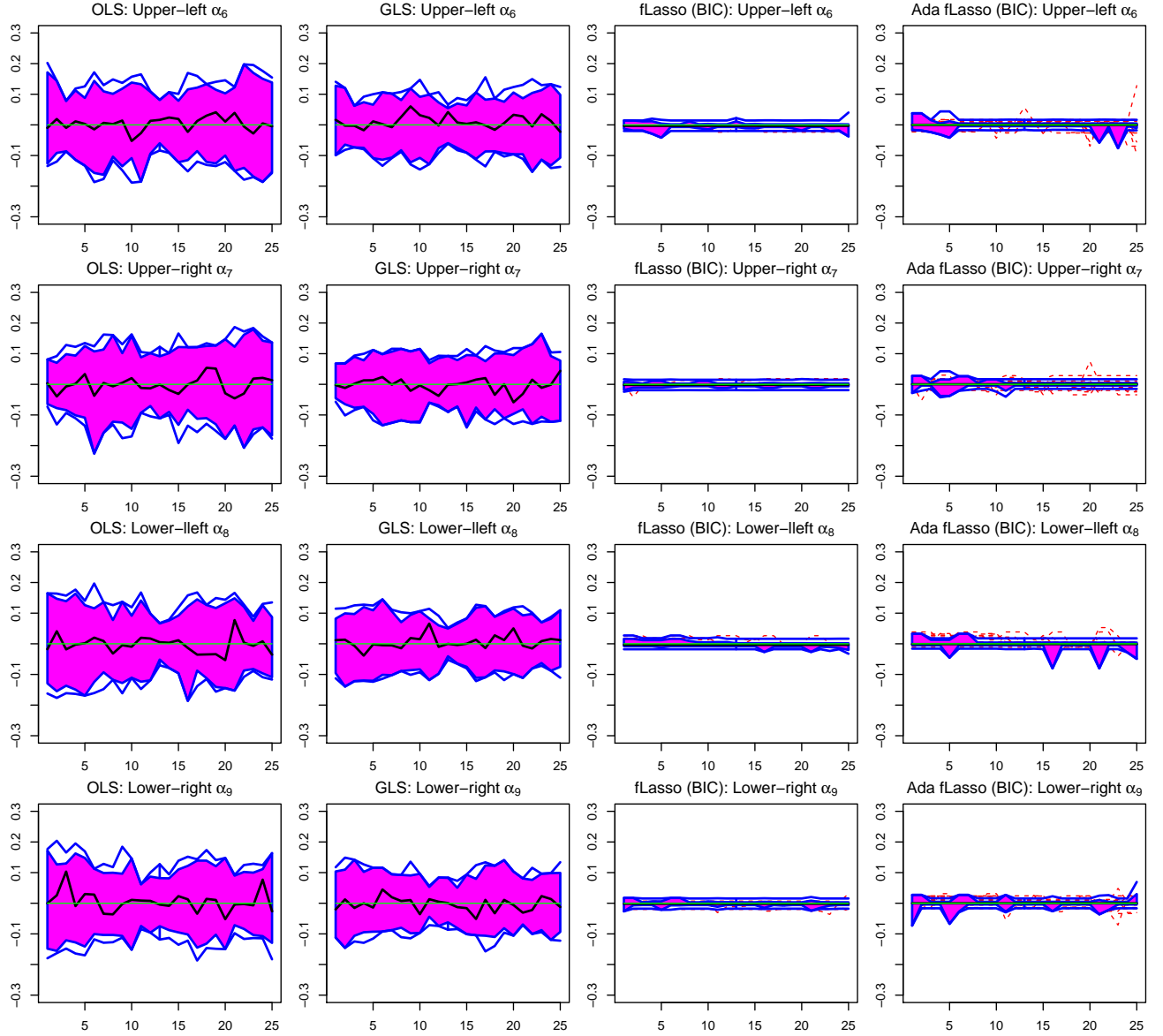


Figure 4: Functional boxplots of the estimated α_k , $k = 6, \dots, 9$ using restricted OLS, restricted GLS, fused Lasso, and adaptive fused Lasso methods with $K = 9$ and $T = 500$ from 500 simulations. True values for α_k are indicated by the green line.

4.3 Forecast Results

We compare the h -step-ahead forecasts of a VAR(1) model for $h = 1, 2, 3$ at all grid points when using the estimated \mathbf{A} by the four methods under consideration (i.e., restricted OLS, restricted GLS, fused Lasso, and adaptive fused Lasso). To measure the forecasting performance, we consider the normalized h -step prediction mean squared error (PMSE), defined as (modified

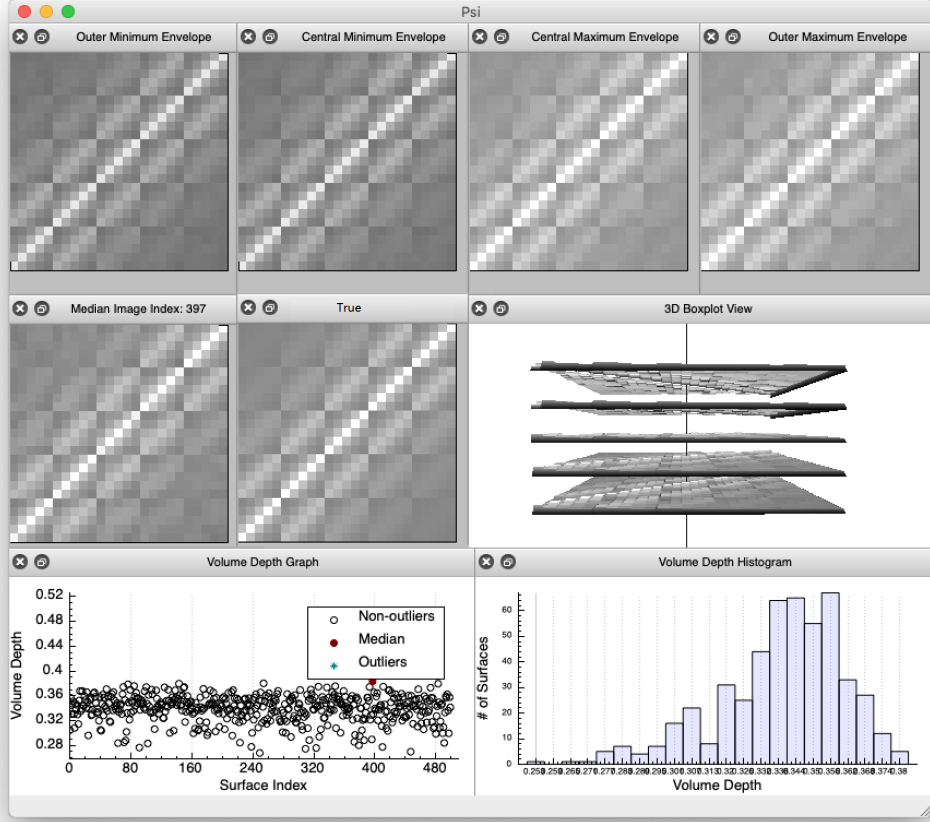


Figure 5: Surface boxplot of the estimated Ψ using our algorithm with $T = 500$ from 500 simulations.

from Hsu et al., 2008):

$$\begin{aligned} \text{PMSE} &= \frac{1}{n} \mathbb{E} \left[(\mathbf{Z}_{t+h} - \hat{\mathbf{Z}}_{t+h})' \boldsymbol{\Sigma}_h^{-1} (\mathbf{Z}_{t+h} - \hat{\mathbf{Z}}_{t+h}) \right] \\ &= 1 + \frac{1}{49} \mathbb{E} \left[(\hat{\mathbf{Z}}_{t+h}^* - \hat{\mathbf{Z}}_{t+h})' \boldsymbol{\Sigma}_h^{-1} (\hat{\mathbf{Z}}_{t+h}^* - \hat{\mathbf{Z}}_{t+h}) \right], \end{aligned} \quad (9)$$

where $\hat{\mathbf{Z}}_{t+h}^*$ and $\hat{\mathbf{Z}}_{t+h}$ are the h -step best linear predictors based on the true and estimated models, respectively, and $\boldsymbol{\Sigma}_h$ is the theoretical h -step prediction variance with the true model. The PMSE for only the inner grid points can be obtained by dividing by 25 instead of 49, and using the sub-vector of $\hat{\mathbf{Z}}_{t+h}^{*(i)}$ and $\hat{\mathbf{Z}}_{t+h}^{(i)}$, and sub-matrix $\boldsymbol{\Sigma}_h$ corresponding to the inner grid points in (9).

Table 1 reports the empirical PMSE based on the four estimation methods for all 49 locations as well as the inner 25 points. We see that forecasts with \mathbf{A} estimated using the adaptive fused

Table 1: PMSE of h -step ahead forecasts for $h = 1, 2, 3$ based on four estimates of \mathbf{A} from 500 simulations for both the 49 locations and the inner 25 points; the standard errors are given in parentheses.

| | h | Restricted OLS | Restricted GLS | Fused Lasso | Adaptive fused Lasso |
|--------------------|-----|---------------------|---------------------|---------------------|----------------------|
| 49 locations | 1 | 1.0060 (0.00012) | 1.0037 (0.00007) | 1.0019 (0.00004) | 1.0011 (0.00003) |
| | 2 | 1.0035 (0.00008) | 1.0022 (0.00004) | 1.0013 (0.00003) | 1.0008 (0.00002) |
| | 3 | 1.0024 (0.00007) | 1.0014 (0.00004) | 1.0009 (0.00003) | 1.0005 (0.00002) |
| 25 inner points | 1 | 1.0099 (0.00021) | 1.0060 (0.00012) | 1.0024 (0.00007) | 1.0010 (0.00004) |
| | 2 | 1.0057 (0.00013) | 1.0036 (0.00008) | 1.0019 (0.00005) | 1.0009 (0.00003) |
| | 3 | 1.0043 (0.00013) | 1.0025 (0.00007) | 1.0016 (0.00005) | 1.0008 (0.00003) |

Lasso always have the smallest PMSE.

5 Application to Daily Wind Speed Data

To illustrate the usefulness of our model, we use a climate model dataset of daily wind speeds over Saudi Arabia. The Large Ensemble Project (LENS) dataset is publicly available and consists of 30 ensembles of daily wind speeds over the globe at a spatial resolution of 1.25° longitude and 0.94° latitude from the year 1920 to 2100 (Kay et al., 2015). We select one ensemble from the dataset and use the historical 86 years (1920-2005) of data at $n = 195$ points, including the gridded locations across the domain of Saudi Arabia, plus one outer layer of the domain to produce the boundary conditions, resulting in a grid irregularly bounded roughly by $15 - 33^\circ\text{N}$ and $34 - 56^\circ\text{E}$. First, we estimate the seasonality of the daily wind speeds at each location by taking the average wind speed across each day of all 86 years at each location. We remove the seasonal effect from each time point and get the residual wind speed for each location. Since the residual daily wind speed is right-skewed, we use the Tukey g -and- h transformation, as in Yan and Genton (2019), to Gaussianize the residuals. We estimate the transformation at each grid point and use the transformed residuals to fit our spatially structured VAR(1) model. Maps of

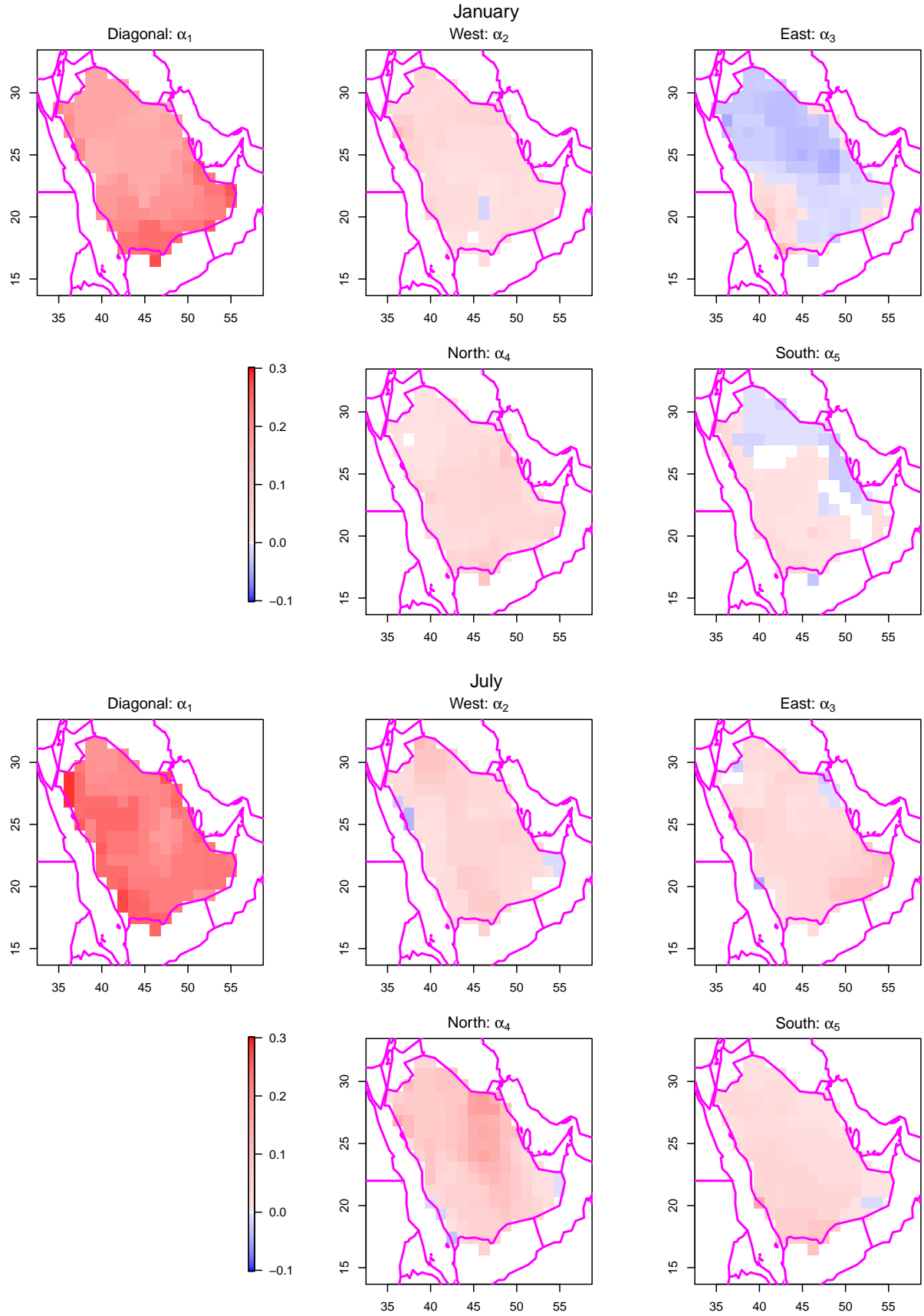


Figure 6: Maps of the estimated autoregressive coefficients using our algorithm (adaptive fused Lasso) with $K = 5$ for the Tukey g -and- h transformed residual daily wind speeds on January and July of 86 years (1920-2005) on a grid covering Saudi Arabia.

the estimated parameters related to the transformation can be found in Yan and Genton (2019).

We use the Gaussianized residual daily wind speeds of January and July in the 86 years ($T = 31 \times 86 = 2666$) to fit our model with $K = 5$, and use our proposed adaptive fused Lasso method to estimate the lagged coefficients. For this grid configuration, we have $n_I = 149$, $n_B = 46$, and hence $m = 791$ for the length of α .

Figure 6 shows the estimation results for the $n_I = 149$ inner grid locations. Comparing maps of these adaptive fused Lasso estimators for January and July, we see distinct patterns of the coefficients. Overall, the autoregressive coefficients of July have larger magnitudes than those of January, which indicate stronger temporal dependencies. The difference can be seen eminently by comparing the coefficients for the northern neighbor between January and July. The stronger dependencies by the northern neighbors in July might be explained by the intensified northerly winds during the monsoon circulation in summer. In January, coefficients for the eastern and southern neighbors have distinct patterns and are slightly negative in the northern part of Saudi Arabia, while in July the patterns are more homogeneous. We also notice that coefficients for coastal locations are not clustered together and exhibit complex patterns. These findings are insightful for explaining the underlying phenomenon. With the estimated parameters, the model can be then used for building stochastic weather generators as an approximation of the computationally expensive climate model.

6 Discussion

In this paper, we introduced VAR models for stationary time series on gridded locations with sparse and spatially coherent autoregressive coefficients to achieve dimension reduction. Our model is interpretable, flexible, and captures the spatial non-stationarity and essential dynamics of spatiotemporal processes. We detailed our model for the VAR(1) case, developed an estimation algorithm and derived its asymptotic properties. By a simulation study, we showed the satisfying performance of our estimation algorithm as well as the advantage in forecasting. As illustrated

by the data example, our model can be used to identify spatial subregions by examining patterns in the estimated coefficients and thus gain insights into the underlying dynamics over space. Also, our model designed for gridded spatial data is particularly suitable for building stochastic weather generators.

For the general VAR(p) case, our model assumes for $j = 1, \dots, p$, the process at each of the $i = 1, \dots, n_I$ inner grid points is directly affected only by the lag- j process at the K_j neighboring locations and can be written as $Z_t(\mathbf{s}_i) = \sum_{k=1}^{K_1} \alpha_{1k}(\mathbf{s}_i) Z_{t-1}(\mathbf{s}_i + \mathbf{u}_k) + \dots + \sum_{k=1}^{K_p} \alpha_{pk}(\mathbf{s}_i) Z_{t-p}(\mathbf{s}_i + \mathbf{u}_k) + \epsilon_t(\mathbf{s}_i)$. Again, this lagged-neighborhood scheme ensures sparsity of each of the transition matrices. Then the homogeneity assumption is on $\boldsymbol{\alpha}_{jk} = (\alpha_{jk}(\mathbf{s}_1), \dots, \alpha_{jk}(\mathbf{s}_{n_I}))'$ for each $j = 1, \dots, p$ and $k = 1, \dots, K_j$. Detailed equations and estimation algorithm can be derived similarly as the VAR(1) case. Instead of using a fixed order p and pre-defined neighboring scheme, order and neighbor selection can be made simultaneously using BIC.

For the boundary points, we assumed a simple AR(1) model in order to provide a dynamic mechanism on the boundary for forecasting. Estimation of the dynamics for the inner grid points should not be affected much by this assumption as it is done conditional on the boundary variables. If several steps ahead forecast is not of interest, then there is no need to specify a model for the boundary points and the likelihood in (5) can be replaced by the likelihood conditioning on the boundary points. In this case the transition matrix is of size $n_I \times n$. Overall, the effect of edge sites specification is a thorny problem in spatial statistics and deserves further investigation.

Our model is suitable for data rich in space with n up to hundreds of locations. For the data example with $n = 195$, our estimation algorithm using the ‘genlasso’ package took about 1 hour on a Dell desktop with a 3.30GHz Intel CPU. However, with very high dimension, the estimation takes much longer and becomes unstable. Therefore, a more efficient and stable algorithm solving the generalized Lasso problem needs to be implemented. For very short time series when $T < n$, the non-parametric estimation of $\boldsymbol{\Psi}$ in (8) results in a singular matrix. In this case, further regularization can be imposed on $\boldsymbol{\Psi}$ or a parametric model can be adopted to estimate $\boldsymbol{\Psi}$, such

as the Matérn covariance family.

In neither our simulation study nor data example did we encounter a case where the estimated \mathbf{A} was non-stable. This potential problem could be dealt with by imposing the stable constraints, e.g., $\sum_{k=1}^K |\alpha_k(\mathbf{s}_i)| \leq 1$, $i = 1, \dots, n_I$. For the non-Gaussian spatiotemporal wind speed data, we estimated the transformation at each location separately. This method could be extended to estimate the parameters related to the transformation and $\boldsymbol{\alpha}$ for the underlying spatially structured Gaussian VAR process simultaneously; in this situation, a fused Lasso penalty would also be imposed on the transformation parameters. At last, observations with measurement error are rarely dealt with for regularized VAR models and could be an interesting topic for further research.

References

- Ailliot, P., Monbet, V., and Prevosto, M. (2006), “An autoregressive model with time-varying coefficients for wind fields,” *Environmetrics*, 17, 107–117.
- Arnold, T. B., and Tibshirani, R. J. (2014), *genlasso: Path algorithm for generalized lasso problems*, R package version 1.3.
- Bañbura, M., Giannone, D., and Reichlin, L. (2010), “Large Bayesian vector auto regressions,” *Journal of Applied Econometrics*, 25, 71–92.
- Basu, S., and Michailidis, G. (2015), “Regularized estimation in sparse high-dimensional time series models,” *The Annals of Statistics*, 43, 1535–1567.
- Bergmeir, C., and Bentez, J. M. (2012), “On the use of cross-validation for time series predictor evaluation,” *Information Sciences*, 191, 192–213.
- Bessac, J., Ailliot, P., and Monbet, V. (2015), “Gaussian linear state-space model for wind fields in the North-East Atlantic,” *Environmetrics*, 26, 29–38.

- Brunsdon, C., Fotheringham, A. S., and Charlton, M. E. (1996), “Geographically Weighted Regression: A Method for Exploring Spatial Nonstationarity,” *Geographical Analysis*, 28, 281–298.
- Cressie, N., and Wikle, C. K. (2011), *Statistics for Spatio-Temporal Data*, Wiley: Hoboken, NJ.
- de Luna, X., and Genton, M. G. (2005), “Predictive spatio-temporal models for spatially sparse environmental data,” *Statistica Sinica*, 15, 547–568.
- Gelfand, A. E., Kim, H.-J., Sirmans, C. F., and Banerjee, S. (2003), “Spatial Modeling With Spatially Varying Coefficient Processes,” *Journal of the American Statistical Association*, 98, 387–396.
- Genton, M., Johnson, C., Potter, K., Stenchikov, G., and Sun, Y. (2014), “Surface boxplots,” *Stat*, 3, 1–11.
- Hsu, N.-J., Hung, H.-L., and Chang, Y.-M. (2008), “Subset selection for vector autoregressive processes using Lasso,” *Computational Statistics and Data Analysis*, 52, 3645–3657.
- Huang, H.-C., Hsu, N.-J., Theobald, D. M., and Breidt, F. J. (2010), “Spatial Lasso With Applications to GIS Model Selection,” *Journal of Computational and Graphical Statistics*, 19, 963–983.
- Katzfuss, M., and Cressie, N. (2012), “Bayesian hierarchical spatio-temporal smoothing for very large datasets,” *Environmetrics*, 23, 94–107.
- Kay, J. E., Deser, C., Phillips, A., Mai, A., Hannay, C., Strand, G., Arblaster, J. M., Bates, S. C., Danabasoglu, G., Edwards, J., Holland, M., Kushner, P., Lamarque, J.-F., Lawrence, D., Lindsay, K., Middleton, A., Munoz, E., Neale, R., Oleson, K., Polvani, L., and Vertenstein, M. (2015), “The Community Earth System Model (CESM) Large Ensemble Project: A Community Resource for Studying Climate Change in the Presence of Internal Climate Variability,” *Bulletin of the American Meteorological Society*, 96, 1333–1349.

- Kazor, K., and Hering, A. S. (2019), “Mixture of Regression Models for Large Spatial Datasets,” *Technometrics*, 61, 507–523.
- Ke, Z. T., Fan, J., and Wu, Y. (2015), “Homogeneity Pursuit,” *Journal of the American Statistical Association*, 110, 175–194.
- Korobilis, D., and Pettenuzzo, D. (2019), “Adaptive hierarchical priors for high-dimensional vector autoregressions,” *Journal of Econometrics*, 212, 241–271.
- Li, F., and Sang, H. (2019), “Spatial Homogeneity Pursuit of Regression Coefficients for Large Datasets,” *Journal of the American Statistical Association*, 114, 1050–1062.
- Monbet, V., and Ailliot, P. (2017), “Sparse vector Markov switching autoregressive models. Application to multivariate time series of temperature,” *Computational Statistics & Data Analysis*, 108, 40–51.
- Ngueyep, R., and Serban, N. (2015), “Large-Vector Autoregression for Multilayer Spatially Correlated Time Series,” *Technometrics*, 57, 207–216.
- R Development Core Team (2019), *R: A Language and Environment for Statistical Computing*, R Foundation for Statistical Computing, Vienna, Austria.
- Rao, S. S. (2008), “Statistical analysis of a spatio-temporal model with location-dependent parameters and a test for spatial stationarity,” *Journal of Time Series Analysis*, 29, 673–694.
- Schweinberger, M., Babkin, S., and Ensor, K. B. (2017), “High-Dimensional Multivariate Time Series With Additional Structure,” *Journal of Computational and Graphical Statistics*, 26, 610–622.
- Shen, X., and Huang, H.-C. (2010), “Grouping Pursuit Through a Regularization Solution Surface,” *Journal of the American Statistical Association*, 105, 727–739.

- Sun, Y., and Genton, M. G. (2011), “Functional Boxplots,” *Journal of Computational and Graphical Statistics*, 20, 316–334.
- Sun, Y., Wang, H. J., and Fuentes, M. (2016), “Fused Adaptive Lasso for Spatial and Temporal Quantile Function Estimation,” *Technometrics*, 58, 127–137.
- Tagle, F., Castruccio, S., Crippa, P., and Genton, M. G. (2019), “A non-Gaussian spatio-temporal model for daily wind speeds based on a multivariate skew- t distribution,” *Journal of Time Series Analysis*, 40, 312–326.
- Tibshirani, R., Saunders, M., Rosset, S., Zhu, J., and Knight, K. (2005), “Sparsity and smoothness via the fused lasso,” *Journal of the Royal Statistical Society: Series B*, 67, 91–108.
- Tibshirani, R. J., and Taylor, J. (2011), “The solution path of the generalized lasso,” *The Annals of Statistics*, 39, 1335–1371.
- Viallon, V., Lambert-Lacroix, S., Höfling, H., and Picard, F. (2013), “Adaptive Generalized Fused-Lasso: Asymptotic Properties and Applications,” Working paper.
- Wikle, C. K., Berliner, L. M., and Cressie, N. (1998), “Hierarchical Bayesian space-time models,” *Environmental and Ecological Statistics*, 5, 117–154.
- Wikle, C. K., Milliff, R. F., Nychka, D., and Berliner, L. M. (2001), “Spatiotemporal Hierarchical Bayesian Modeling: Tropical Ocean Surface Winds,” *Journal of the American Statistical Association*, 96, 382–397.
- Yan, Y., and Genton, M. G. (2019), “Non-Gaussian autoregressive processes with Tukey g -and- h transformations,” *Environmetrics*, 30, e2503.
- Zou, H. (2006), “The Adaptive Lasso and Its Oracle Properties,” *Journal of the American Statistical Association*, 101, 1418–1429.

A Appendix

Proof of Lemma 1: It suffices to show that the modulus for any eigenvalue of \mathbf{A} is less than 1. We prove this by contradiction. We assume that \mathbf{A} has an eigenvector $\mathbf{v} = (v_1, \dots, v_n)' \in \mathbb{C}^n$ with the corresponding eigenvalue $\lambda \in \mathbb{C}$ such that $|\lambda| \geq 1$. We let v_i be the element of \mathbf{v} with the largest modulus. The i th element of $\mathbf{A}\mathbf{v}$ is $\sum_{j=1}^n a_{ij}v_j$; its modulus is $|\sum_{j=1}^n a_{ij}v_j| \leq \sum_{j=1}^n |a_{ij}||v_j| < |v_i|$ since $\sum_{j=1}^n |a_{ij}| < 1$. However, the i th element of $\lambda\mathbf{v}$ is λv_i , which has a modulus of $|\lambda v_i| > |v_i|$. This contradicts the assumption that $\mathbf{A}\mathbf{v} = \lambda\mathbf{v}$. \square

Derivation of (5):

$$l(\boldsymbol{\alpha}) = -\frac{1}{2} \sum_{t=2}^T \mathbf{Z}'_{t-1} \mathbf{A}' \boldsymbol{\Psi}^{-1} \mathbf{A} \mathbf{Z}_{t-1} + \sum_{t=2}^T \mathbf{Z}'_t \boldsymbol{\Psi}^{-1} \mathbf{A} \mathbf{Z}_{t-1} + \text{constant}.$$

For the two terms involved in the above equation,

$$\begin{aligned} \sum_{t=2}^T \mathbf{Z}'_t \boldsymbol{\Psi}^{-1} \mathbf{A} \mathbf{Z}_{t-1} &= \text{vec} \left(\boldsymbol{\Psi}^{-1} \sum_{t=2}^T \mathbf{Z}_t \mathbf{Z}'_{t-1} \right)' \text{vec}(\mathbf{A}) = \text{vec} \left(\boldsymbol{\Psi}^{-1} \sum_{t=2}^T \mathbf{Z}_t \mathbf{Z}'_{t-1} \right)' \mathbf{P} \boldsymbol{\alpha}, \text{ and} \\ \sum_{t=2}^T \mathbf{Z}'_{t-1} \mathbf{A}' \boldsymbol{\Psi}^{-1} \mathbf{A} \mathbf{Z}_{t-1} &= \text{vec}(\mathbf{A})' \left\{ \left(\sum_{t=1}^{T-1} \mathbf{Z}_t \mathbf{Z}'_t \right) \otimes \boldsymbol{\Psi}^{-1} \right\} \text{vec}(\mathbf{A}) = \boldsymbol{\alpha}' \mathbf{P}' \left\{ \left(\sum_{t=1}^{T-1} \mathbf{Z}_t \mathbf{Z}'_t \right) \otimes \boldsymbol{\Psi}^{-1} \right\} \mathbf{P} \boldsymbol{\alpha}. \end{aligned}$$

Then, it is easy to see that the log-likelihood is a quadratic form of $\boldsymbol{\alpha}$, i.e.:

$$l(\boldsymbol{\alpha}) = -\frac{1}{2} \|\mathbf{y} - \mathbf{X}\boldsymbol{\alpha}\|_2^2 + \text{constant},$$

where \mathbf{X} and \mathbf{y} satisfy (3) and (4). \square

Proof of Theorem 1: The following proof is obtained by adapting the Proof of Theorem 2 in Zou (2006) and Theorem 3 in Viallon et al. (2013).

We define $V_T(\mathbf{u}) = F(\boldsymbol{\alpha}^0) - F(\boldsymbol{\alpha}^0 + \mathbf{u}/\sqrt{T})$, with F defined in (6). It is obvious that $V_T(\mathbf{u})$ is minimized at $\sqrt{T}(\hat{\boldsymbol{\alpha}} - \boldsymbol{\alpha}^0)$ and

$$V_T(\mathbf{u}) = \mathbf{u}' \left(\frac{1}{2T} \mathbf{X}' \mathbf{X} \right) \mathbf{u} - \frac{\boldsymbol{\xi}' \mathbf{X}}{\sqrt{T}} \mathbf{u} + \frac{\lambda}{\sqrt{T}} \sum_{(i,j) \in \mathcal{A}} w_{i,j} \sqrt{T} \left(\left| \alpha_i^0 - \alpha_j^0 + \frac{u_i - u_j}{\sqrt{T}} \right| - |\alpha_i^0 - \alpha_j^0| \right).$$

We have

$$\lambda w_{i,j} \left| \alpha_i^0 - \alpha_j^0 + \frac{u_i - u_j}{\sqrt{T}} \right| - |\alpha_i^0 - \alpha_j^0| \xrightarrow{p} \begin{cases} 0, & \text{if } \alpha_i^0 \neq \alpha_j^0 \text{ or } (\alpha_i^0 = \alpha_j^0 \text{ and } u_i = u_j), \\ \infty, & \text{otherwise.} \end{cases}$$

We denote $\mathbf{u}_{\mathcal{A}} = (\mathbf{u}_{l_1}, \dots, \mathbf{u}_{l_{m_0}})'$ and then, with an application of the Martingale difference central limit theory to $\boldsymbol{\xi}' \mathbf{X}$, we obtain

$$V_T(\mathbf{u}) \xrightarrow{d} V(\mathbf{u}) = \begin{cases} \frac{1}{2} \mathbf{u}'_{\mathcal{A}} \mathbf{C}_{\mathcal{A}} \mathbf{u}_{\mathcal{A}} - \mathbf{u}'_{\mathcal{A}} \mathbf{W}_{\mathcal{A}}, & \text{if } u_i = u_j \text{ for } (i, j) \in \mathcal{A}, \\ \infty, & \text{otherwise,} \end{cases}$$

for $\mathbf{u} \in \mathbb{R}^m$, where $\mathbf{W}_{\mathcal{A}} \sim \mathcal{N}_m(\mathbf{0}, \mathbf{C}_{\mathcal{A}})$; V is convex and has a unique minimum satisfying $u_i = u_j$ for all $(i, j) \in \mathcal{A}$ and $\mathbf{u}_{\mathcal{A}} = \mathbf{C}_{\mathcal{A}}^{-1} \mathbf{W}_{\mathcal{A}}$. The asymptotic normality part can be derived as in Zou (2006) by using the epi-convergence results.

For consistency in grouping, we need to show that for all $(i, j) \notin \mathcal{A}$, $\Pr((i, j) \in \mathcal{A}_n^c) \rightarrow 1$ and for all $(i, j) \in \mathcal{A}$, $\Pr((i, j) \in \mathcal{A}_n^c) \rightarrow 0$. The first part is implied by the asymptotic normality result. To prove the second part, we apply the subgradient equations for the optimality condition, for $i = 1, \dots, m$:

$$\mathbf{X}'_i(\mathbf{y} - \mathbf{X}\hat{\boldsymbol{\alpha}}) = \lambda \sum_{i:(i,j) \in \mathcal{E}} w_{i,j} t_{ij},$$

where $t_{ij} = \text{sign}(\hat{\alpha}_i - \hat{\alpha}_j)$ if $\hat{\alpha}_i \neq \hat{\alpha}_j$ and t_{ij} is some real number in $[-1, 1]$ if $\hat{\alpha}_i = \hat{\alpha}_j$. We prove by contradiction. Suppose that for \mathcal{V}_k that contains at least two vertices, there exist $i, j \in \mathcal{V}_k$ such that $\hat{\alpha}_i \neq \hat{\alpha}_j$. We define $a^{\min} = \min_{i \in \mathcal{V}_k} \hat{\alpha}_i$ and $\mathcal{V}^{\min} = \{i : i \in \mathcal{V}_k \text{ and } \hat{\alpha}_i = a^{\min}\}$. Summing up the optimality conditions over the indices in \mathcal{V}^{\min} , we get:

$$\sum_{i \in \mathcal{V}^{\min}} \frac{\mathbf{X}'_i(\mathbf{y} - \mathbf{X}\hat{\boldsymbol{\alpha}})}{\sqrt{T}} = \frac{\lambda}{\sqrt{T}} \sum_{i \in \mathcal{V}^{\min}} \sum_{\substack{i:(i,j) \in \mathcal{E} \\ \alpha_i^0 \neq \alpha_j^0}} \frac{t_{ij}}{|\tilde{\alpha}_i - \tilde{\alpha}_j|^{\gamma}} + \lambda T^{(\gamma-1)/2} \sum_{i \in \mathcal{V}^{\min}} \sum_{\substack{i:(i,j) \in \mathcal{E} \\ \alpha_i^0 = \alpha_j^0 \\ \hat{\alpha}_j > a^{\min}}} \frac{t_{ij}}{|\sqrt{T}(\tilde{\alpha}_i - \tilde{\alpha}_j)|^{\gamma}},$$

where in the right-hand side, the first sum converges to 0 in probability, while the second sum tends to $-\infty$. However, the left-hand side is $O_p(1)$, since it can be decomposed as the sum of two asymptotically normal variables as in Zou (2006) with an application of the martingale central limit theorem. Therefore $\Pr((i, j) \in \mathcal{A}_n^c) \rightarrow 0$. \square